



Negative Hall coefficient of ultrathin niobium in Si/Nb/Si trilayers

I. Zaytseva,¹ O. Abal'oshev,¹ P. Dłuzewski,¹ W. Paszkowicz,¹ L. Y. Zhu,² C. L. Chien,²
M. Kończykowski,³ and Marta Z. Cieplak¹

¹*Institute of Physics, Polish Academy of Sciences, 02 668 Warsaw, Poland*

²*Department of Physics and Astronomy, The Johns Hopkins University, Baltimore, Maryland 21218, USA*

³*Laboratoire des Solides Irradies, École Polytechnique, 91128 Palaiseau, France*

(Received 22 July 2014; revised manuscript received 11 August 2014; published 22 August 2014)

Structural and transport properties of thin Nb layers in Si/Nb/Si trilayers with Nb layer thickness d from 1.1 nm to 50 nm have been studied. With decreasing thickness, the structure of the Nb layer changes from polycrystalline to amorphous at $d \simeq 3.3$ nm, while the superconducting temperature T_c monotonically decreases. The Hall coefficient varies with d systematically but changes sign into negative in ultrathin films with $d < 1.6$ nm. The influence of boundary scattering on the relaxation rate of carriers, and band broadening in the amorphous films, may contribute to this effect.

DOI: [10.1103/PhysRevB.90.060505](https://doi.org/10.1103/PhysRevB.90.060505)

PACS number(s): 74.62.En, 74.25.F–

The properties of ultrathin superconducting films differ from those of the bulk material. One of the best known examples is the decrease of the superconducting transition temperature T_c with decrease of film thickness, accompanied by the increase of the normal-state film resistance [1–12]. Many factors may influence thin-film properties. The enhanced density of defects or large boundary scattering may reduce the mean-free path of the carriers, the electron-electron and electron-phonon interactions may become different from those in bulk materials, and the structural properties may be affected by the strain or interdiffusion, thus modifying the electronic band structure. The establishing of which of these factors plays a major role is important both for the understanding of superconductivity in the ultrathin limit and for the successful application of these films in novel devices. Many studies have been devoted to this subject. However, in most of them the transport evaluation is limited to the resistance or magnetoresistance measurements, while the Hall effect is rarely investigated.

In this work we study ultrathin niobium (Nb) films, and we show that the measurements of the Hall coefficient provide unexpected insights into ultrathin film properties. Nb has the highest T_c among elemental superconductors and is widely used in many investigations and applications. The properties of thin Nb films have been addressed by numerous studies, with particular emphases on the dependence of the T_c on the film thickness [2,6–12]. These studies already show that the thin film fabrication process and the substrate strongly influence the film properties. The Nb films grown on sapphire at elevated temperatures often have superior superconducting properties [8,9,12], but may suffer from interdiffusion between the substrate and the film [9,12]. On the other hand, in Nb films made by magnetron sputtering at room temperature [10,11] interdiffusion should be absent, and such films are an excellent choice for many applications [13]. Here we focus on the films prepared by the second method.

In addition to superconducting properties, we show that there are other subtle changes in Nb thin films as one systematically decreases film thickness, including structure transformation and the evolution of the resistance per square (R_{sq}). Most surprisingly, there is also a change of sign in

the Hall coefficient (R_H) from positive to negative in ultrathin Nb films, suggesting two types of carriers contributing to conduction. This raises the question of its role in the disappearance of superconductivity in the thinnest films.

The Nb films of thickness d , from 1.1 nm to 50 nm, sandwiched between two Si layers of 10 nm to prevent oxidation, have been made by magnetron sputtering at room temperature on glass substrates. We have verified by secondary ion mass spectrometry that the Si buffer layer between the substrate and Nb is necessary to avoid diffusion of oxygen from glass into Nb. We have also determined that the Si overlayer does not affect the T_c of Nb, indicating negligible proximity effect between Nb and Si, as has been reported [14]. The Nb film thickness was controlled by deposition time after the deposition rate has been established from low-angle x-ray reflectivity measurements. In addition, a control set of Si/Nb/Si trilayers with different d has been deposited on the Si wafers, for imaging by the high-resolution transmission electron microscopy (HRTEM). From these images, small differences between the nominal and actual d values have been found for ultrathin films. The actual d values are used here.

In addition to the HRTEM imaging, we use x-ray diffraction to evaluate the structural properties of the trilayers. The resistance per square, R_{sq} , as a function of temperature is measured on a lithographically patterned resistance bridge using a standard four-probe method. The Hall coefficient R_H is measured on the patterned “Hall bar” structure, using a physical property measurement system (PPMS; Quantum Design). In addition, the measurements of R_H using the van der Pauw method have been done for some of the (unpatterned) samples. The results obtained by two methods are found to agree within experimental accuracy.

Figure 1 shows the x-ray diffraction patterns of several trilayers with different d , and of a reference sample with two buffer Si layers but without the niobium layer in between ($d = 0$). A single broad maximum situated at low angle, characteristic for an amorphous material, is visible in the pattern of the reference sample. On the other hand, the pattern for film with $d = 11.3$ nm reveals diffraction peaks consistent with the bcc crystal structure and space group $Im\bar{3}m$ of Nb

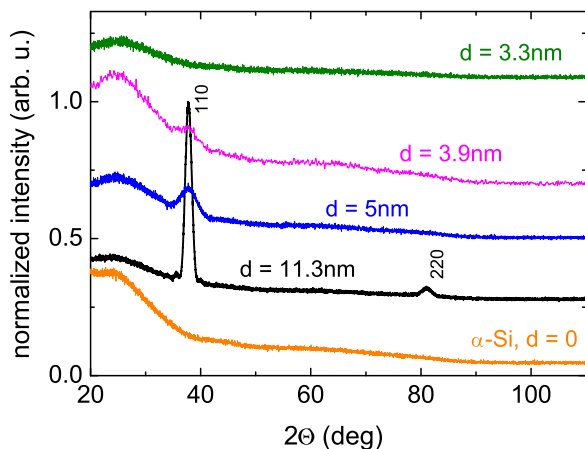


FIG. 1. (Color online) X-ray diffraction spectra for the Si/Nb(d)/Si trilayers with different thickness d indicated in the figure. The consecutive curves are shifted vertically for clarity.

with the lattice parameter of 3.36 ± 0.01 Å, slightly larger than the value of 3.294 Å for bulk Nb. With d decreasing to 5 nm the intensity of the diffraction peaks decreases, and the peaks become substantially broadened. At $d = 3.9$ nm only one peak is still faintly visible. This suggests that the film still contain some polycrystalline grains, but a substantial portion of the film is amorphous. Finally, at $d = 3.3$ nm there is no evidence of any crystalline phase.

Figure 2 shows HRTEM images for trilayers with different d . The Nb layer (dark) is sandwiched between amorphous Si layers (light), and the growth direction is from top to bottom. The Nb/Si boundaries are sharp, suggesting little or no diffusion of Si into Nb. The images (b) and (c) show that thin niobium layers are amorphous throughout the whole thickness. In the thick sample [image (a)] we observe a layer of amorphous niobium, about 1.5 nm thick, situated at the top Si/Nb boundary. Apparently, during the initial stage of deposition niobium forms amorphous layer. However, after a sufficiently thick film has been deposited, crystalline grains begin to form, of the lateral size of about 3 nm, as indicated by the area

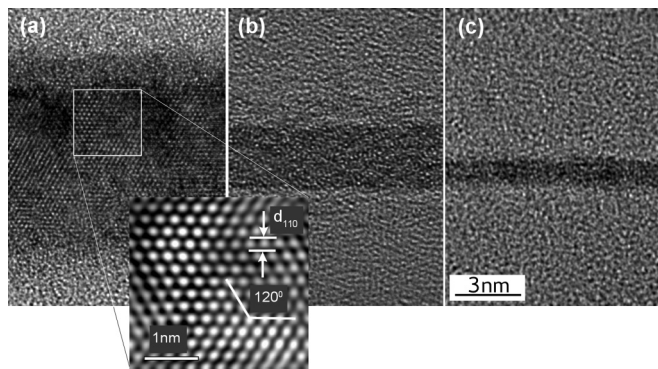


FIG. 2. HRTEM images for Si/Nb(d)/Si trilayers, with d equal to 11.3 nm (a), 3.3 nm (b), and 1.2 nm (c). The layers in images are (from the top) amorphous Si, niobium, and amorphous Si. The inset at the bottom shows the enlarged Fourier-filtered part of image (a) indicated by the white square.

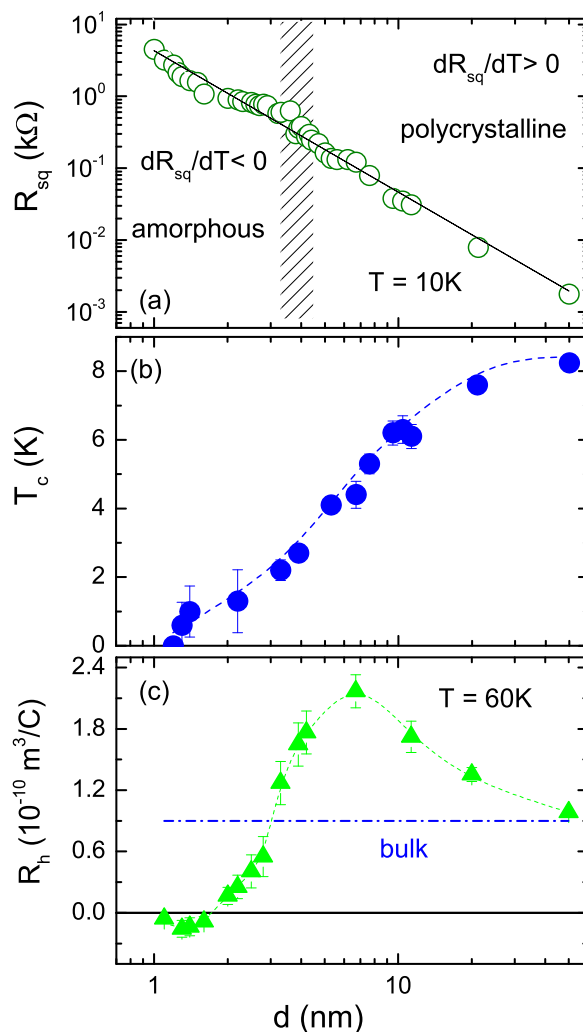


FIG. 3. (Color online) R_{sq} (a), T_c (b), and R_H at $T = 60$ K (c) vs film thickness d . In (a) the continuous line shows the fitted dependence $R_{sq} \sim d^{-2}$, and the hatched area indicates the transition region between the polycrystalline and amorphous films. In (b) and (c) the dashed lines are guides to the eye.

enclosed by the white square. The Fourier filtered HRTEM image of this grain, shown in the bottom inset, confirms the bcc structure with $\langle 111 \rangle$ orientation. With further deposition of Nb, the grains coalesce, forming continuous polycrystalline film with good structural alignment [15]. Similar formation of amorphous Nb layer at the Si/Nb interface, about 1–2 nm thick, has been reported in case of Si/Nb superlattices [16].

The dependence of R_{sq} on d at $T = 10$ K is shown in Fig. 3(a). The data follow approximately the power law $R_{sq} \sim d^{-2}$, as indicated by a straight line fitted to the data. Such dependence has been predicted for the size effect, resulting either from film-boundary scattering in single-crystalline thin films [17,18] or from a combination of grain-boundary and film-boundary scattering in polycrystalline films [19], and it has been observed before in both types of Nb films [2,7,9]. Thus, it appears that in our polycrystalline films the boundary scattering may be an important scattering mechanism. Interestingly, same dependence seems to extend to amorphous films,

in which grain boundaries are absent and the mean-free path is short. It is possible that in this case some other factors, dependent on the film thickness, affect the R_{sq} , such as the enhanced defect density. We note also that the T dependence of R_{sq} changes with d , so that we observe $dR_{sq}/dT > 0$ for thick films, and $dR_{sq}/dT < 0$ for ultrathin films. The transition between these two limits, indicated in the figure by dashed area at $d \simeq 4$ nm, correlates approximately with the transition region between the polycrystalline and the amorphous films.

The influence of d on the T_c is shown in Fig. 3(b). Here T_c is the midpoint of the superconducting transition and the vertical error bars reflect 90% to 10% transition width. The T_c decreases to zero for $d \simeq 1.3$ nm when R_{sq} exceeds about 1800 Ω , but in the film with $d = 1.2$ nm we still see the evidence of superconducting fluctuations. The dependence of $T_c(R_{sq})$ is similar to the one reported for Nb films prepared by other methods [7,11], as will be discussed later.

Figure 3(c) shows the R_H , measured at $T = 60$ K, versus d . We observe that in the thickest films the R_H is close to the value for the bulk, equal to 0.9×10^{-10} m³/C [20]. With decreasing d the R_H initially increases above the bulk value. According to theories, the boundary scattering should result in the increase of the Hall coefficient [18]. However, when d decreases below 6 nm, the R_H starts to decrease. Eventually, it changes sign into negative for very thin films, when d decreases below 1.6 nm.

The change of sign in the thinnest samples is further enhanced when temperature is decreased. To emphasize this we show in Fig. 4 the evolution the Hall resistance R_{xy} with increasing B , measured at various temperatures for samples with different d . We observe several features. First, the slope of the $R_{xy}(B)$ dependence changes dramatically, from positive in the thicker sample shown in (a) to negative in the thinnest amorphous sample shown in (c). Second, with the decrease of temperature the slope increases in both cases, but while in (a) it becomes more positive, in (c) it becomes more negative; this feature will be discussed in more detail below. Finally, in the thinnest sample the $R_{xy}(B)$ dependence becomes slightly nonlinear at the lowest temperatures. This nonlinearity is even more visible in the case of the intermediate sample, $d = 2$ nm, shown in (b). The $R_{xy}(B)$ is linear with positive slope at high T , but as T is lowered nonlinearity gradually develops, until at $T = 2$ K a negative slope appears at small B .

To illustrate better the second feature described above, we extract the R_H from the linear $R_{xy}(B)$ dependencies. The results are shown in Fig. 5, where we plot the variation with T of the quantity $\Delta R_H/R_H^{300}$, where $\Delta R_H(T) \equiv R_H(T) - R_H^{300}$ is defined as a relative change of the R_H with respect to the room-temperature value, R_H^{300} . We observe that in all samples the absolute value of ΔR_H increases with the decreasing T . However, while ΔR_H is positive in the thick samples, it is negative in the ultrathin films. The change of sign from positive into negative ΔR_H occurs for $d \simeq 2.8$ nm, indicating that for all thinner samples the Hall coefficient is reduced with decreasing T .

All the features listed above strongly suggest that the conduction in the ultrathin Nb layers involves contribution from two types of carriers, holes and electrons. While holes dominate the transport in thicker, polycrystalline samples, similar as it is in bulk niobium, the negative electron contribution

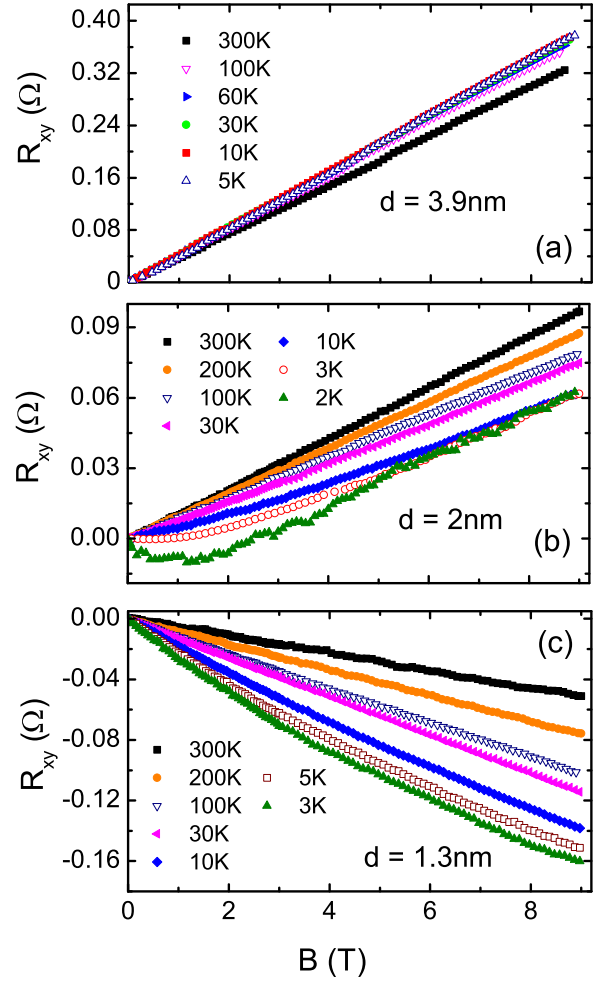


FIG. 4. (Color online) Hall resistance R_{xy} versus B at different temperatures for samples with $d = 3.9$ nm (a), $d = 2$ nm (b), and $d = 1.3$ nm (c).

becomes increasingly important as d decreases; it is also more pronounced at low T . Due to small electron effective mass the negative contribution dominates at low magnetic fields, while in the limit of large fields the positive hole contribution

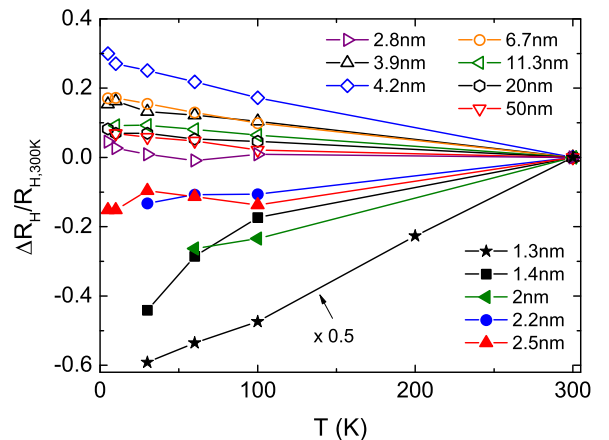


FIG. 5. (Color online) $\Delta R_H/R_H^{300}$ versus T for trilayers with different d . The data for $d = 1.3$ nm are multiplied by 0.5.

prevails. The exception is the thinnest film, with $d = 1.3$ nm, for which the magnetic field used in our experiment may be too small to observe hole contribution.

The electron contribution to the conduction in the thin-film limit may have several origins. One possibility is that in the thin amorphous films the Nb band structure is modified, so that the character of the dominating carriers changes. However, this effect alone cannot be the cause, because the films become purely amorphous for $d = 3.3$ nm, while R_H is still positive and comparable to the bulk value, so there is no strict correlation between these two effects.

Another possible origin is the formation of silicide niobium layer at the Nb/Si interface [21], which may exhibit negative R_H [22]. Such a layer may be very thin and amorphous, and therefore undetectable by our experimental methods. The conduction could proceed via two parallel conduction channels with carriers of different signs, with the effect becoming stronger as d decreases.

Still another possibility is the effect described for polycrystalline films of indium, in which a change of sign of R_H , from positive in thick films to a negative in the low-field limit in thin films, has been reported [23–25]. It is explained by the influence of boundary scattering on the relaxation times of the two types of carriers which exist in In, i.e., the heavy holes in the second Brillouin zone and light electrons in the third zone [20]. In the bulk the R_H is positive, because the relaxation time for holes is larger than for electrons, which are more strongly scattered by impurities. The boundary scattering in thin films affects similarly both types of carriers, tending to equalize the relaxation rates, and electron contribution becomes evident at low magnetic fields.

Trying to assess whether such mechanism may exist in Nb, we note that the Fermi surface in bcc niobium consists of closed-hole surface in the second zone, while in the third zone there are distorted hole ellipsoids and an open multiply connected surface known as the “jungle gym,” which may support both hole and electron orbits [26,27]. In the bulk the electron orbits do not affect R_H , but when d decreases, the boundary scattering may gradually uncover the electron contribution. While this mechanism is likely to be present in polycrystalline films, in amorphous films, without grain boundaries and with short mean-free path, it is probably less efficient. It is possible that some other, d -dependent scattering mechanism [evident from $R_{sq}(d)$ dependence] may additionally affect the relaxation rates. Finally, the band broadening in the amorphous films may play some role.

It is intriguing to ask to a what extent our finding of electron contribution to transport may modify the understanding of the suppression of superconductivity in ultrathin Nb films. To comment on this we examine in Fig. 6 the dependence of T_c/T_{c0} on the normal-state sheet resistance R_{sq} for the whole set of trilayers with different d . Here $T_{c0} = 9.22$ K is the T_c of the bulk niobium, and the R_{sq} is measured at the onset of superconducting transition. We also plot by continuous lines the predictions of theoretical model proposed by Finkel’stein [28] for homogeneously disordered films, which takes into account the fact that disorder diminishes screening of the Coulomb interactions between carriers. The model includes parameter $\gamma = \ln(\frac{h}{k_B T_{c0} \tau})$, where k_B is the

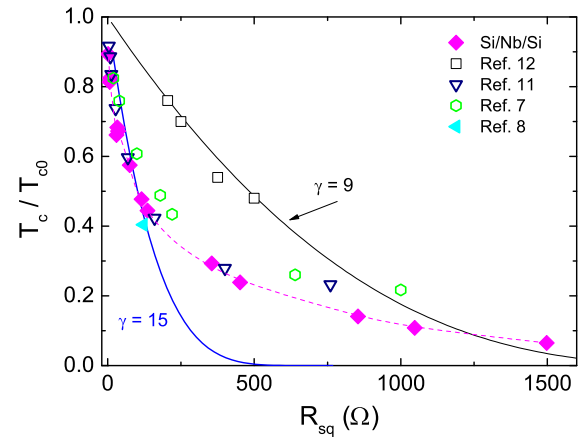


FIG. 6. (Color online) The ratio T_c/T_{c0} versus normal-state sheet resistance R_{sq} for Si/Nb/Si trilayers with different d (full magenta squares) and for several different sets of Nb films prepared by other methods, Ref. [12] (open black squares), Ref. [11] (open blue triangles), Ref. [7] (open green diamonds), and Ref. [8] (full cyan triangle). The dashed magenta line is a guide to the eye. The predictions of the Finkel’stein model are shown by continuous lines, for $\gamma = 9$ (black) and $\gamma = 15$ (blue).

Boltzmann constant and τ is the elastic diffusion time. The plots of two curves, for γ equal 15 and 9, indicate that the theoretical predictions with a single value of γ cannot describe correctly the data in the full range of R_{sq} . While reasonable description is obtained for samples with $R_{sq} \lesssim 200$ Ω , for thinner samples the decrease of the T_c with increasing of R_{sq} slows down. The important observation is that the limiting value of $R_{sq} \simeq 200$ Ω occurs for $d \simeq 5$ nm, below which the electron contribution to the conductance begins to affect the Hall coefficient. Thus, a possibility exists that in thinner samples the scattering of electron carriers contributes strongly to the increase of R_{sq} , but it does not contribute (or contributes weakly) to the pair breaking. Such situation may occur if the electron carriers are not involved in superconductivity.

Finally, the question arises of whether our findings are limited to the particular set of Nb layers studied here. We cannot answer this definitely, because the Hall coefficient has not been evaluated in previous studies of thin Nb films. However, we may compare the $T_c(R_{sq})$ dependence for our samples and similar data for different sets of Nb films deposited on various substrates using different technological methods [7,8,11,12]. As seen in Fig. 6, most of the data follow the trend similar to that found in present study, i.e., initial fast decrease of the T_c for small R_{sq} , followed by long “tail” for samples with large R_{sq} . The only exception is the set studied in Ref. [12], which appears to be distinctly different, and it is well described by theory using $\gamma = 9$. The smaller value of γ implies larger elastic diffusion time, which is reasonable, because these are the single-crystalline films grown at much higher temperature (660°C) than all the remaining film sets. On the other hand, the similarity between the results for our trilayers and the other previously studied Nb films may suggest that the electron contribution is a general phenomenon which appears in sufficiently disordered films.

In conclusion, we have studied the properties of ultrathin Nb films in the Si/Nb/Si trilayers. We show that Nb films are amorphous for $d < 3.3$ nm. In the thinnest amorphous films we observe a change of the sign of the Hall coefficient into negative, possibly due to the influence of boundary scattering and other d -dependent scattering mechanisms, on the relaxation rate of carriers. The band structure modification in the amorphous films may also be important.

We are grateful to A. Malinowski and V. Bezusyy for their involvement in setting up the PPMS apparatus. This work has been supported by Polish NSC Grant No. 2011/01/B/ST3/00462, by NSF Grant No. DMR 1262253, and by the French-Polish Bilateral Program PICS 2012. The research was partially performed in two laboratories co-financed by the ERDF Projects POIG.02.01-00-14-032/08 and NanoFun POIG.02.02.00-00-025/09.

-
- [1] J. E. Crow and M. Strongin, *Phys. Rev. B* **3**, 2365 (1971).
 [2] A. F. Mayadas, R. B. Laibowitz, and J. J. Cuomo, *J. Appl. Phys.* **43**, 1287 (1972).
 [3] J. M. Graybeal and M. R. Beasley, *Phys. Rev. B* **29**, 4167 (1984).
 [4] R. C. Dynes, A. E. White, J. M. Graybeal, and J. P. Garno, *Phys. Rev. Lett.* **57**, 2195 (1986).
 [5] D. B. Haviland, Y. Liu, and A. M. Goldman, *Phys. Rev. Lett.* **62**, 2180 (1989).
 [6] J. H. Quateman, *Phys. Rev. B* **34**, 1948 (1986).
 [7] S. I. Park and T. H. Geballe, *Phys. Rev. Lett.* **57**, 901 (1986).
 [8] J. W. P. Hsu and A. Kapitulnik, *Phys. Rev. B* **45**, 4819 (1992).
 [9] K. Yoshii, H. Yamamoto, K. Saiki, and A. Koma, *Phys. Rev. B* **52**, 13570 (1995).
 [10] A. I. Gubin, K. S. Il'in, S. A. Vitusevich, M. Siegel, and N. Klein, *Phys. Rev. B* **72**, 064503 (2005).
 [11] T. R. Lemberger, I. Hetel, J. W. Knepper, and F. Y. Yang, *Phys. Rev. B* **76**, 094515 (2007).
 [12] C. Delacour, L. Ortega, M. Faucher, T. Crozes, T. Fournier, B. Pannetier, and V. Bouchiat, *Phys. Rev. B* **83**, 144504 (2011).
 [13] A. Semenov, A. Engel, K. Il'in, G. Gol'tsman, M. Siegel, and H.-W. Hübers, *Eur. Phys. J.: Appl. Phys.* **21**, 171 (2003).
 [14] W. M. van Huffelen, T. M. Klapwijk, and E. P. Th. M. Suurmeijer, *Phys. Rev. B* **47**, 5151 (1993).
 [15] Note that the thickness of amorphous layer in thick films is 1.5 nm; i.e., it is smaller than the limiting thickness $d = 3.3$ nm, below which deposited films are amorphous. It is possible that once the polycrystalline grains start to form in thick films, some of the amorphous material, already present on the substrate, crystallizes, thus decreasing the thickness of the amorphous layer.
 [16] S. N. Song, D. X. Li, and J. B. Ketterson, *J. Appl. Phys.* **66**, 5360 (1989).
 [17] K. Fuchs, *Math. Proc. Cambridge Philos. Soc.* **34**, 100 (1938).
 [18] E. H. Sondheimer, *Phys. Rev.* **80**, 401 (1950).
 [19] A. F. Mayadas and M. Shatzkes, *Phys. Rev. B* **1**, 1382 (1970).
 [20] C. M. Hurd, *The Hall Effect in Metals and Alloys* (Plenum Press, New York, 1972).
 [21] G. Wiech, W. Zachorowski, A. Šimůnek, and O. Šipr, *J. Phys. Condens. Matter* **1**, 5595 (1989).
 [22] K. Pomoni, Ch. Krontiras, and J. Saimi, *Appl. Phys.* **23**, 354 (1990).
 [23] J. N. Cooper, P. Cotti, and F. B. Rasmussen, *Phys. Lett.* **19**, 560 (1965).
 [24] J. C. Garland, *Phys. Rev.* **185**, 1009 (1969).
 [25] I. Holwech, *Philos. Mag.* **12**, 117 (1965).
 [26] L. F. Mattheiss, *Phys. Rev. B* **1**, 373 (1970).
 [27] A. R. Jani, N. E. Brener, and J. Callaway, *Phys. Rev. B* **38**, 9425 (1988).
 [28] A. Finkelstein, *JETP Lett.* **45**, 46 (1987); *Physica B: Condens. Matter* **197**, 636 (1994).